

1 A sub-canopy structure for simulating oil palm in the Community Land Model (CLM-Palm):
2 phenology, allocation and yield

3 Yuanchao Fan^{1,2,*}, Olivier Roupsard^{3,4}, Martial Bernoux⁵, Gueric Le Maire³, Oleg Panferov⁶,
4 Martyna M. Kotowska⁷, Alexander Knohl¹

5 ¹ University of Göttingen, Department of Bioclimatology, B üsigenweg 2, 37077 Göttingen,
6 Germany

7 ² AgroParisTech, SIBAGHE (Syst èmes int égr és en Biologie, Agronomie, G éosciences,
8 Hydrosociences et Environnement), 34093 Montpellier, France

9 ³ CIRAD, UMR Eco&Sols (Ecologie Fonctionnelle & Biog éochimie des Sols et des Agro-
10 éosyst èmes), 34060 Montpellier, France

11 ⁴ CATIE (Tropical Agricultural Centre for Research and Higher Education), 7170 Turrialba,
12 Costa Rica

13 ⁵ IRD, UMR Eco&Sols, 34060 Montpellier, France

14 ⁶ University of Applied Sciences Bingen, 55411 Bingen am Rhein, Germany

15 ⁷ University of Göttingen, Department of Plant Ecology and Ecosystems Research, Untere
16 Karsp üle 2, 37073 Göttingen, Germany

17 *Correspondence author. E-mail: yfan1@uni-goettingen.de

18

19 **Abstract:** Towards an effort to quantify the effects of forests to oil palm conversion
20 occurring in the tropics on land-atmosphere carbon, water and energy fluxes, we introduce a
21 new perennial crop phenology and allocation sub-model (CLM-Palm) for simulating a palm
22 plant functional type (PFT) within the framework of the Community Land Model. The CLM-
23 Palm is tested here on oil palm only but is meant of generic interest for other palm crops (e.g.
24 coconut). The oil palm has monopodial morphology and sequential phenology of around 40
25 stacked phytomers, each carrying a large leaf and a fruit bunch, forming a natural multilayer
26 canopy. A sub-canopy phenological and physiological parameterization is thus developed, so
27 that each phytomer has its own prognostic leaf growth and fruit yield capacity but with shared
28 stem and root components. Phenology and carbon and nitrogen allocation operate on the
29 different phytomers in parallel but at unsynchronized steps, separated by a thermal period. An
30 important phenological phase is identified for the oil palm - the storage growth period of bud
31 and “spear” leaves which are photosynthetically inactive before expansion. Agricultural
32 practices such as transplanting, fertilization, and leaf pruning are represented. Parameters
33 introduced for the oil palm were calibrated and validated with field measurements of leaf area
34 index (LAI) and yield from Sumatra, Indonesia. In calibration with a mature oil palm
35 plantation, the cumulative yields from 2005 to 2014 matched notably well between simulation
36 and observation (mean percentage error = 3%). Simulated inter-annual dynamics of PFT-level
37 and phytomer-level LAI were both within the range of field measurements. Validation from
38 eight independent oil palm sites shows the ability of the model to adequately predict the
39 average leaf growth and fruit yield across sites but also indicates that seasonal dynamics and
40 small-scale site-to-site variability of yield are driven by processes not yet implemented in the
41 model or reflected in the input data. The new sub-canopy structure and phenology and
42 allocation functions in CLM-Palm allow exploring the effects of tropical land use change,
43 from natural ecosystems to oil palm plantations, on carbon, water and energy cycles and
44 regional climate.

45 **1. Introduction**

46 Land-use changes in South-East Asia's tropical regions have been accelerated by economy-
47 driven expansion of oil palm (*Elaeis guineensis*) plantations since the 1990s (Miettinen et al.,
48 2011). Oil palm is currently one of the most rapidly expanding crops in the world (Carrasco et
49 al., 2014) and Indonesia as the largest global palm-oil producer is planning to double its oil-
50 palm area from 9.7 million ha in 2009 to 18 million ha by 2020 (Koh and Ghazoul, 2010).

51 Since oil palms favor a tropical-humid climate with consistently high temperatures and
52 humidity, the plantation expansion has converted large areas of rainforest in Indonesia in the
53 past two decades including those on carbon-rich peat soils (Carlson et al., 2012; Gunarso et al.
54 2013).

55 Undisturbed forests have long-lasting capacity to store carbon in comparison to disturbed or
56 managed vegetation (Luysaert et al., 2008). Tropical deforestation caused by the expansion
57 of oil palm plantations has significant implications on above- and belowground carbon stocks
58 (Kotowska et al., 2015a). However, the exact quantification of the forest – oil palm
59 replacement effects is difficult as the greenhouse gas balance of oil palms is still uncertain
60 due to incomplete monitoring of the dynamics of oil palm plantations (including young
61 development stage), and lack of understanding of the carbon, nitrogen, water and energy
62 exchange between oil palms, soil and the atmosphere at ecosystem scale. Besides that, the
63 assessment of these processes in agricultural ecosystems is complicated by human activities
64 e.g. crop management, including planting and pruning, irrigation and fertilization, litter and
65 residues management, and yield outputs. One of the suitable tools for evaluating the feedback
66 of oil palm expansion is ecosystem modelling. Although a series of agricultural models exist
67 for simulating the growth and yield of oil palm such as OPSIM (van Kraalingen et al., 1989),
68 ECOPALM (Combres et al., 2013), APSIM-Oil Palm (Huth et al., 2014), PALMSIM
69 (Hoffmann et al., 2014), these models did not aim yet at the full picture of carbon, water and
70 energy exchanges between land and atmosphere and remain to be coupled with climate

71 models. Given the current and potential large-scale deforestation driven by the expansion of
72 oil palm plantations, the ecosystem services such as yield, carbon sequestration, microclimate,
73 energy and water balance of this new managed oil palm landscape have to be evaluated in
74 order to estimate the overall impact of land-use change on environment including regional
75 and global climate.

76 Land surface modelling has been widely used to characterize the two-way interactions
77 between climate and human activities in terrestrial ecosystems such as deforestation,
78 agricultural expansion, and urbanization (Jin and Miller, 2011; Oleson et al., 2004). A variety
79 of land models have been adapted to simulate land-atmosphere energy and matter exchanges
80 for major crops such as the CLM, LPJmL, JULES, ORCHIDEE models, etc. The Community
81 Land Model (CLM4.5) is the land component of the Community Earth System Model (CESM)
82 (Oleson et al., 2013). The model represents the crop and naturally vegetated land units as
83 patches of plant functional types (PFTs) defined by their key ecological functions (Bonan et
84 al., 2002). However, most of the crops being simulated are annual crops such as wheat, corn,
85 soybean, rice, etc. Their phenological cycles are usually represented as three stages of
86 development from planting to leaf emergence, to fruit-fill and to harvest, all within a year.
87 Attempts were also made to evaluate the climate effects of perennial crops, e.g. by extending
88 the growing season of annuals (Georgescu et al., 2011). However the perennial crops such as
89 oil palm, cacao, coffee, rubber, coconut, and other fruiting trees and their long-term
90 biophysical processes are not represented in the above land models yet, despite the worldwide
91 growing demand (FAO, 2013).

92 Oil palm is a perennial evergreen crop which can be described by the Corner's architectural
93 model (Hall et al., 1978). A number of phytomers, each carrying a large leaf and axillating a
94 fruit bunch, emerge successively (nearly two per month) from a single meristem (the bud) at
95 the top of a solitary stem. They form a multilayer canopy with old leaves progressively being
96 covered by new ones, until being pruned at senescence. Each phytomer has its own

97 phenological stage and yield, according to respective position in the crown. The oil palm is
98 productive for more than 25 years, including a juvenile stage of around 2 years. In order to
99 capture the inter- and intra-annual dynamics of growth and yield and land-atmosphere energy,
100 water and carbon fluxes in the oil palm system, a new structure and dimension detailing the
101 phytomer-level phenology, carbon (C) and nitrogen (N) allocation and agricultural
102 managements have to be added to the current integrated plant-level physiological
103 parameterizations in the land models. This specific refinement needs to remain compliant
104 with the current model structure though, and be simple to parameterize.

105 In this context, we develop a new CLM-Palm sub-model for simulating the growth, yield, and
106 energy and material cycling of oil palm within the framework of CLM4.5. It introduces a sub-
107 canopy phenological and physiological parameterization, so that multiple leaf and fruit
108 components operate in parallel but at delayed steps. A phytomer in the model is meant to
109 represent the average condition of an age-cohort of actual oil palm phytomers across the
110 whole plantation landscape. The overall gross primary production (GPP) by leaves and carbon
111 output by fruit harvests rely on the development trends of individual phytomers. The
112 functions implemented for oil palm combine the characteristics of both trees and crops, such
113 as the woody-like stem growth and turnover but the crop-like vegetative and reproductive
114 allocations which enable fruit C and N output. Agricultural practices such as transplanting,
115 fertilization, and leaf pruning are also represented.

116 The main objectives of this paper are to: i) describe the development of CLM-Palm including
117 its phenology, carbon and nitrogen allocation, and yield output; ii) optimize model parameters
118 using field-measured leaf area index (LAI) and observed long-term monthly yield data from a
119 mature oil palm plantation in Sumatra, Indonesia; and iii) validate the model against
120 independent data from eight oil palm plantations of different age in Sumatra, Indonesia.

121 **2. Model development**

122 For adequate description of oil palm functioning, we adapted the CLM crop phenology,
123 allocation and vegetative structure subroutines to the monopodial morphology and sequential
124 phenology of oil palm so that each phytomer evolves independently in growth and yield (Fig.
125 1). Their phenology sequence is determined by the phyllochron (the period in thermal time
126 between initiations of two subsequent phytomers) (Table A1). A maximum of 40 phytomers
127 and expanded leaves, each growing up to 7-m long, are usually maintained in plantations by
128 pruning management. There are also around 60 initiated phytomers developing slowly inside
129 the bud. The largest ones, already emerged at the top of the crown but unexpanded yet, are
130 named “spear” leaves (Fig. 1a). Each phytomer can be considered a sub-PFT component that
131 has its own prognostic leaf growth and fruit yield capacity but having 1) the stem and root
132 components that are shared by all phytomers, 2) the soil water content, nitrogen resources,
133 and resulting photosynthetic assimilates that are also shared and partitioned among all
134 phytomers, and 3) a vertical structure of the foliage, with the youngest at the top and the
135 oldest at the bottom of the canopy. Within a phytomer the fruit and leaf components do not
136 compete for growth allocation because leaf growth usually finishes well before fruit-fill starts.
137 However one phytomer could impact the other ones through competition for assimilates,
138 which is controlled by the C and N allocation subroutine according to their respective
139 phenological stages.

140 Here we describe only the new phenology, allocation and agricultural management functions
141 developed for the oil palm. Photosynthesis, respiration, water and nitrogen cycles and other
142 biophysical processes already implemented in CLM4.5 (Oleson et al., 2013) are not modified
143 (except N retranslocation scheme) for the current study. The following diagram shows the
144 new functions and their coupling with existing modules within the CLM4.5 framework (Fig.
145 2).

146 **2.1. Phenology**

147 Establishment of the oil palm plantation is implemented with two options: seed sowing and
148 transplanting of seedlings. In this study, only the transplanting option is used. We design 7
149 phenological steps for the development of each phytomer: 1) leaf initiation; 2) start of leaf
150 expansion; 3) leaf maturity; 4) start of fruit-fill; 5) fruit maturity and harvest; 6) start of leaf
151 senescence; and 7) end of leaf senescence and pruning (Fig. 1b). The first two steps
152 differentiate pre-expansion (heterotrophic) and post-expansion (autotrophic) leaf growth
153 phases. The other steps control leaf and fruit developments independently so that leaf growth
154 and maturity could be finished well before fruit-fill and leaf senescence could happen after
155 fruit harvest according to field observations. The modified phenology subroutine controls the
156 life cycle of each phytomer as well as the planting, stem and root turnover, vegetative
157 maturity (start of fruiting) and final rotation (replanting) of the whole PFT. Details on the
158 timing and implementation of oil palm phenology and nitrogen retranslocation during
159 senescence are in the Supplementary materials. The main phenological parameters are in
160 Table A1.

161 All phytomers are assumed to follow the same phenological steps, where the thermal length
162 for each phase is measured by growing degree-days (GDD; White et al., 1997). For oil palm,
163 a new GDD variable with 15 °C base temperature and 25 degree-days daily maximum (Corley
164 and Tinker, 2003; Goh, 2000; Hormaza et al., 2012) is accumulated from planting (abbr.
165 GDD₁₅). The phenological phases are signaled by respective GDD requirements, except that
166 pruning is controlled by the maximum number of live phytomers according to plantation
167 management (Table A1). Other processes in the model such as carbon and nitrogen allocation
168 for growth of new tissues respond to this phenology scheme at both PFT level and phytomer
169 level (section 2.2).

170 **2.2. Carbon and Nitrogen allocation**

171 In CLM, the fate of newly assimilated carbon from photosynthesis is determined by a coupled
172 C and N allocation routine. Potential allocation for new growth of various plant tissues is
173 calculated based on allocation coefficients and their allometric relationship (Table A2).

174 A two-step allocation scheme is designed for the sub-canopy phytomer structure and
175 according to the new phenology. First, available C (after subtracting respiration costs) is
176 partitioned to the root, stem, overall leaf, and overall fruit pools at the PFT level with respect
177 to their relative demands controlled by phenology. The C:N ratios for different tissues link C
178 demand and N demand so that a N down-regulation mechanism is enabled to rescale GPP and
179 C allocation if N availability from soil mineral N pool and retranslocated N pool does not
180 meet the demand. Then, the actual C and N allocated to the overall leaf or fruit is partitioned
181 between different phytomers at the sub-PFT level (Fig. 2). Details are described below.

182 2.2.1. PFT level allocation

183 C and N allocation at the PFT level is treated distinctly before and after oil palm reaches
184 vegetative maturity. At the juvenile stage before fruiting starts (i.e. $GDD_{15} < GDD_{min}$) all the
185 allocation goes to the vegetative components. The following equations are used to calculate
186 the fractions of available C and N allocated to the leaf, stem, and root pools.

$$187 \quad A_{root} = a_{root}^i - (a_{root}^i - a_{root}^f) \frac{DPP}{Age_{max}}, \quad (\text{Eq. 1})$$

$$188 \quad A_{leaf} = f_{leaf}^i \times (1 - A_{root}) \quad (\text{Eq. 2})$$

$$189 \quad A_{stem} = 1 - A_{root} - A_{leaf} \quad (\text{Eq. 3})$$

190 where $\frac{DPP}{Age_{max}} \leq 1$, DPP is the days past planting, and Age_{max} is the maximum plantation age
191 (~25 years). a_{root}^i and a_{root}^f are the initial and final allocation coefficients for roots and f_{leaf}^i

192 is the initial leaf allocation coefficient before fruiting (Table A2). Root and stem allocation
 193 ratios are calculated with Eqs. 1 and 3 for all ages and phenological stages of oil palm.

194 After fruiting begins, the new non-linear function is used for leaf allocation:

$$195 \quad A_{leaf} = a_{leaf}^2 - (a_{leaf}^2 - a_{leaf}^f) \left(\frac{DPP - DPP_2}{Age_{max} \times d_{mat} - DPP_2} \right)^{d_{alloc}^{leaf}} \quad (\text{Eq. 4})$$

196 where a_{leaf}^2 equals the last value of A_{leaf} calculated right before fruit-fill starts and DPP_2 is
 197 the days past planting right before fruit-fill starts. d_{mat} controls the age when the leaf
 198 allocation ratio approaches its final value a_{leaf}^f , while d_{alloc}^{leaf} determines the shape of change
 199 (convex when $d_{alloc}^{leaf} < 1$; concave when $d_{alloc}^{leaf} > 1$). A_{leaf} stabilizes at a_{leaf}^f when $DPP \geq$
 200 $Age_{max} d_{mat}$. The equations reflect changed vegetative allocation strategy that shifts
 201 resources to leaf for maintaining LAI and increasing photosynthetic productivity when
 202 fruiting starts. The three vegetative allocation ratios A_{leaf} , A_{stem} and A_{root} always sum to 1.

203 At the reproductive phase a fruit allocation ratio A_{fruit} is introduced, relative to the total
 204 vegetative allocation unity. To represent the dynamics of reproductive allocation effort of oil
 205 palm, we adapt the stem allocation scheme for woody PFTs in CLM, in which increasing net
 206 primary production (NPP) results in increased allocation ratio for the stem wood (Oleson et
 207 al., 2013). A similar formula is used for reproductive allocation of oil palm so that it increases
 208 with increasing NPP:

$$209 \quad A_{fruit} = \frac{2}{1 + e^{-b(NPP_{mon} - 100)}} - a \quad (\text{Eq. 5})$$

210 where NPP_{mon} is the monthly sum of NPP from the previous month calculated with a run-
 211 time accumulator in the model. The number 100 (gC/m²/mon) is the base monthly NPP when
 212 the palm starts to yield (Kotowska et al., 2015a). Parameters a and b adjust the base allocation
 213 rate and the slope of curve, respectively (Table A2). This function generates a dynamic curve

214 of A_{fruit} increasing from the beginning of fruiting to full vegetative maturity ($0 \leq A_{fruit} \leq$
 215 2), which is used in the allocation allometry to partition assimilates between vegetative and
 216 reproductive pools (Fig. 3).

217 2.2.2. Sub-PFT (phytomer) level allocation

218 Total leaf and fruit allocations are partitioned to the different phytomers according to their
 219 phenological stages. Fruit allocation per phytomer is calculated with a sink size index:

$$220 \quad S_p^{fruit} = \frac{GDD_{15} - H_p^{F.fill}}{H_p^{F.mat} - H_p^{F.fill}}, \quad (\text{Eq. 6})$$

221 where p stands for the phytomer number, $H_p^{F.fill}$ and $H_p^{F.mat}$ are the phenological indices for
 222 the start of fruit-fill and fruit maturity (with $H_p^{F.fill} \leq GDD_{15} \leq H_p^{F.mat}$). S_p^{fruit} increases
 223 from zero at the beginning of fruit-fill to the maximum of 1 right before harvest for each
 224 phytomer. This is because the oil palm fruit accumulates assimilates at increasing rate during
 225 development until the peak when it becomes ripe and oil synthesis dominates the demand
 226 (Corley and Tinker, 2003). The sum of S_p^{fruit} for all phytomers gives the total reproductive
 227 sink size index. Each phytomer receives a portion of fruit allocation by $\frac{S_p^{fruit}}{\sum_{p=1}^n S_p^{fruit}} \times A_{fruit}$,
 228 where A_{fruit} is the overall fruit allocation by Eq. 5.

229 An important allocation strategy for leaf is the division of displayed versus storage pools for
 230 the pre-expansion and post-expansion leaf growth phases. These two types of leaf C and N
 231 pools are distinct in that only the displayed pools contribute to LAI growth, whereas the
 232 storage pools support the growth of unexpanded phytomers, i.e. bud & spear leaves, which
 233 remain photosynthetically inactive. Total C and N allocation to the overall leaf pool is divided
 234 to the displayed and storage pools by a fraction lf_{disp} (Table A2) according to the following
 235 equation:

236
$$\begin{aligned} A_{leaf}^{display} &= lf_{disp} \times A_{leaf} \\ A_{leaf}^{storage} &= (1 - lf_{disp}) \times A_{leaf} \end{aligned} \quad (\text{Eq. 7})$$

237 The plant level $A_{leaf}^{display}$ and $A_{leaf}^{storage}$ are then distributed evenly to expanded and
 238 unexpanded phytomers, respectively, at each time step. When a phytomer enters the leaf
 239 expansion phase, C and N from its leaf storage pools transfer gradually to the displayed pools
 240 during the expansion period. Therefore, a transfer flux is added to the real-time allocation flux
 241 and they together contribute to the post-expansion leaf growth.

242 LAI is calculated only for each expanded phytomer according to a constant specific leaf area
 243 (SLA) and prognostic amount of leaf C accumulated by phytomer n . In case it reaches the
 244 prescribed maximum ($PLAI_{max}$), partitioning of leaf C and N allocation to this phytomer
 245 becomes zero.

246 **2.3. Other parameterizations**

247 Nitrogen retranslocation is performed exclusively during leaf senescence and stem turnover.
 248 A part of N from senescent leaves and from the portion of live stem that turns dead is
 249 remobilized to a separate N pool that feeds plant growth or reproductive demand. Nitrogen of
 250 fine roots is all moved to the litter pool during root turnover. We do not consider N
 251 retranslocation from live leaves, stem and roots specifically during grain-fill that is designed
 252 for annual crops (Drewniak et al., 2013) because oil palm has continuous fruit-fill year around
 253 at different phytomers.

254 The fertilization scheme for oil palm is adapted to the plantation management generally
 255 carried out in our study area, which applies fertilizer biannually, starting only 6 years after
 256 planting, assuming each fertilization event lasts one day. Currently CLM uses an
 257 unrealistically high denitrification rate under conditions of nitrogen saturation, e.g. after
 258 fertilization, which results in a 50% loss of any excess soil mineral nitrogen per day (Oleson

259 et al., 2013). This caused the simple biannual regular fertilization nearly useless because peak
260 N demand by oil palm is hard to predict given its continuous fruiting and vegetative growth
261 and most fertilized N is thus lost in several days. The high denitrification factor has been
262 recognized as an artifact (Drewniak et al., 2013; Tang et al., 2013). According to a study on a
263 banana plantation in the tropics (Veldkamp and Keller, 1997), around 8.5% of fertilized N is
264 lost as nitrogen oxide (N_2O and NO). Accounting additionally for a larger amount of
265 denitrification loss to gaseous N_2 , we modified the daily denitrification rate from 0.5 to 0.001,
266 which gives a 30% annual loss of N due to denitrification that matches global observations
267 (Galloway et al., 2004).

268 The irrigation option is turned off because oil palm plantations in the study area are usually
269 not irrigated. Other input parameters for oil palm such as its optical, morphological, and
270 physiological characteristics are estimated based on a literature review and field observations
271 and summarized in Table A3. Most of them are generalized over the life of oil palm.

272 **3. Model evaluation**

273 **3.1. Site data**

274 Two oil palm plantations in the Jambi province of Sumatra, Indonesia provide data for
275 calibration. One is a mature industrial plantation at PTPN-VI (01 °41.6' S, 103 °23.5' E, 2186
276 ha) planted in 2002, which provides long-term monthly harvest data (2005 to 2014). Another
277 is a 2-year young plantation at a nearby smallholder site Pompa Air (01 °50.1' S, 103 °17.7' E,
278 5.7 ha). The leaf area and dry weight at multiple growth stages were measured by sampling
279 leaflets of phytomers at different ranks (+1 to +20) on a palm and repeating for 3 different
280 ages within the two plantations. The input parameter SLA (Table A2) was derived from leaf
281 area and dry weight (excluding the heavy rachis). The phytomer-level LAI was estimated
282 based on the number of leaflets (90-300) per leaf of a certain rank and the PFT-level LAI was
283 estimated by the number of expanded leaves (35-45) per palm of a certain age. In both cases,

284 a planting density of 156 palms per hectare (8m × 8m per palm) was used according to
285 observation.

286 Additionally, LAI, yield and NPP measurements from eight independent mature oil palm sites
287 (50m × 50m each, > 10 years old) were used for model validation. Four of these sites (HO1,
288 HO2, HO3, HO4) are located in the Harapan region nearby PTPN-VI, and another four (BO2,
289 BO3, BO4, BO5) are located in Bukit Duabelas region (02°04' S, 102°47' E), both in Jambi,
290 Sumatra. Fresh bunch harvest data were collected at these sites for a whole year from July
291 2013 to July 2014. Harvest records from both PTPN-VI and the 8 validation sites were
292 converted to harvested carbon (g C/m²) with mean wet/dry weight ratio of 58.65 % and C
293 content 60.13 % per dry weight according to C:N analysis (Kotowska et al., 2015a). The oil
294 palm monthly NPP and its partitioning between fruit, leaf, stem and root were estimated
295 based on measurements of fruit yield (monthly), pruned leaves (monthly), stem increment
296 (every 6 month) and fine root samples (once in a interval of 6-8 month) at the eight sites
297 (Kotowska et al., 2015b).

298 The mean annual rainfall (the Worldclim database: <http://www.worldclim.org> (Hijmans et al.,
299 2005); average of 50 years) of the two investigated landscapes in Jambi Province was ~2567
300 mm y⁻¹ in the Harapan region (including PTPN-VI) and ~2902 mm y⁻¹ in the Bukit Duabelas
301 region. In both areas, May to September represented a markedly drier season (30% less
302 precipitation) in comparison to the rainy season between October and April. Air temperature
303 is relatively constant throughout the year with an annual average of 26.7 °C. In both
304 landscapes, the principal soil types are Acrisols: in the Harapan landscape loam Acrisols
305 dominate, whereas in Bukit Duabelas the majority is clay Acrisol. Soil texture such as
306 sand/silt/clay ratios and soil organic matter C content were measured at multiply soil layers
307 (down to 2.5m) (Allen et al., 2015). They were used to create two sets of surface input data
308 for the Harapan (H) and Bukit Duabelas (B) regions separately.

309 **3.2. Model setup**

310 The model modifications and parameterizations were implemented according to CLM
311 standards. A new sub-PFT dimension called *phytomer* was added to all the new variables so
312 that the model can output history tapes of their values for each phytomer and prepare restart
313 files for model stop and restart with bit-for-bit continuity. Simulations were set up in point
314 mode (a single 0.5×0.5 degree grid) at every 30-min time step. A spin-up procedure (Koven et
315 al., 2013) was followed to get a steady-state estimate of soil C and N pools before 1850, with
316 broadleaf evergreen tropical forest PFT only. Simulation continued on this equilibrium
317 condition but was forced with dynamic CO₂ and climate data until 1990. After 1990, the
318 forest was replaced with the oil palm at a specific year of plantation establishment. The oil
319 palm functions were then turned on and simulations continued until 2014.

320 A simulation from 2002 to 2014 at the PTPN-VI site was used for model calibration.
321 Additional eight simulations were run for the sites HO1, HO2, HO3, HO4, BO2, BO3, BO4,
322 BO5 with two types of surface input files (for soil texture) and two types of climate forcing
323 files (3-hourly ERA Interim data, Dee et al., 2011) for the H and B plots, respectively. The
324 simulations started from different years (1996, 1997, 1999, 2000, 2001, 2002, 2003, 2004)
325 when the palms were planted at the individual sites. Outputs from these simulations were used
326 to validate the model in terms of LAI and yield.

327 **3.3. Calibration of key parameters**

328 Both the PFT level and phytomer level LAI development were calibrated with field
329 observations in 2014 from a chronosequence approach (space for time substitution) using oil
330 palm samples of three different age and multiple phytomers of different rank (section 3.1).
331 Simulated yield outputs (around twice per month) were calibrated with monthly harvest
332 records of PTPN-VI plantation from 2005 to 2014. Cumulative yields were compared because
333 the timing of harvest in the plantations was largely uncertain and varied depending on
334 weather and other conditions.

335 To simplify model calibration, we focused on parameters related to the new phenology and
336 allocation processes. Phenological parameters listed in Table A1 were determined according
337 to field observations and existing knowledge about oil palm growth phenology (Combres et
338 al., 2013; Corley and Tinker, 2003) as well as plantation management in Sumatra, Indonesia.
339 Allocation coefficients in Table A2 were more uncertain and they were the key parameters to
340 optimize in order to match observed LAI and yield dynamics.

341 Parameters related to photosynthesis, stomatal conductance and respirations were set at
342 similar levels as those of other crops, except that leaf traits such as $PLAI_{max}$ and SLA were
343 determined by field measurements. Other parameters such as C:N ratios of the leaf, stem, root
344 and fruit components were also left as similar levels as other crop PFTs.

345 **3.4. Sensitivity analysis**

346 Performing a full sensitivity analysis of all parameters used in simulating oil palm (more than
347 100 parameters, though a majority are shared with natural vegetation and other crops) would
348 be a challenging work. As with calibration, we limited the sensitivity analysis to a set of
349 parameters introduced for the specific PFT and model structure designed for oil palm. Among
350 the phenological parameters, $mxlivenp$ and $phyllochron$ (see Table A1) are closely related to
351 pruning frequency but they should not vary widely for a given oil palm breed and plantation
352 condition. Therefore, they were fixed at the average level for the study sites in Jambi,
353 Sumatra. GDD_{init} was kept to zero because only the transplanting scenario was considered for
354 seedling establishment. We tested two hypotheses of phytomer level leaf development based
355 on the other phenological parameters: 1) considering the leaf storage growth period, that is,
356 the bud & spear leaf phase is explicitly simulated with the GDD parameter values in Table A1
357 and $lf_{disp} = 0.3$ in Table A2; 2) excluding the storage growth period by setting $GDD_{exp} = 0$ and
358 $lf_{disp} = 1$ so that leaf expands immediately after initiation and leaf C and N allocation all goes
359 to the photosynthetic active pools.

360 The sensitivity of allocation and photosynthesis parameters in Table A2 were tested by adding
361 or subtracting 10% or 30% to the baseline values (calibrated) one-by-one and calculating their
362 effect on final cumulative yield at the end of simulation (December 2014). In fact, all the
363 allocation parameters are interconnected because they co-determine photosynthesis capacity
364 and respiration costs as partitioning to the different vegetative and reproductive components
365 varies. This simple approach provides a starting point to identify sensitive parameters,
366 although a more sophisticated sensitivity analysis is needed in the future.

367 Parameter $PLAI_{max}$ is only meant for error controlling, although in our simulations phytomer-
368 level LAI never reached $PLAI_{max}$ (see Fig. 5 in results) because environmental constraints and
369 nitrogen down-regulation already limited phytomer leaf growth well within the range. The
370 C:N ratios and some photosynthesis and respiration parameters were evaluated thoroughly in
371 Billionis et al. (2015). Since we do not consider specific N retranslocation during fruit-fill,
372 some C:N parameters are not used for oil palm and the aspect of N content in different plant
373 tissues is not prioritized for this sensitivity analysis.

374 **3.5. Validation**

375 In this study, we only validated the model structure and model behavior on simulating
376 aboveground C partitioning and flux as represented by LAI, fruit yield and NPP. Independent
377 LAI, yield and monthly NPP data collected in 2013–2014 from the eight mature oil palm sites
378 (H and B plots) were compared with eight simulations using the above model settings and
379 calibrated parameters.

380 **4. Results**

381 **4.1. Calibration with LAI and yield**

382 In model calibration with the PTPN-VI plantation, the PFT-level LAI dynamics simulated by
383 the model incorporating the pre-expansion phase matches well with the LAI measurements

384 for three different ages (Fig. 4). Simulated LAI for the PFT increases with age in a sigmoid
385 relationship. The dynamics of LAI is also impacted by pruning and harvest events because oil
386 palms invest around half of their assimilates into fruit yield. Oil palms are routinely pruned by
387 farmers to maintain the maximum number of expanded leaves around 40. Hence, when yield
388 begins 2-3 years after planting, LAI recurrently shows an immediate drop after pruning and
389 then quickly recovers. Simulations without the pre-expansion storage growth phase show an
390 unrealistic fast increase of LAI before 3 years old, much higher than observed in the field. At
391 older age after yield begins, LAI drops drastically and recovers afterwards. Although the final
392 LAI could stabilize at a similar level, the initial jump and drop of LAI at young stage do not
393 match field observations and cannot be solved by adjusting parameters other than GDD_{exp} .
394 Hereafter, all simulations were run using the pre-expansion phase.

395 The phytomer level LAI development is comparable with leaf samples from the field (Fig. 5).
396 The two leaf samples at rank 5 (LAI = 0.085) and rank 20 (LAI = 0.122) of a mature oil palm
397 in PTPN-VI (the two black triangles for 2014) are within the range of simulated values. The
398 other sample at rank 25 (LAI = 0.04, for 2004) on a young oil palm in Pompa Air is lower
399 than the simulated value. Each horizontal color bar clearly marks the post-expansion leaf
400 phenology cycle, including gradual increment of photosynthetic LAI during phytomer
401 development and gradual declining during senescence. The pre-expansion phase is not
402 included in the figure but model outputs show that roughly 60-70% of leaf C in a phytomer is
403 accumulated before leaf expansion, which is co-determined by the allocation ratio $l_{f_{disp}}^f$ and
404 the lengths of two growth phases set by GDD_{exp} and $GDD_{L.mat}$. This is comparable to
405 observations on coconut palm that dry mass of the oldest unexpanded leaf accounts for 60%
406 of that of a mature leaf (Navarro et al., 2008). Only when the palm becomes mature,
407 phytomer LAI could come closer to the prescribed $PLAI_{max}$ (0.165). However, during the
408 whole growth period from 2002 to 2014 none of the phytomers have reached $PLAI_{max}$, which
409 is the prognostic result of the carbon balance simulated by the model.

410 The cumulative yield of baseline simulation has overall high consistency with harvest records
411 (Fig. 6). The mean percentage error (MPE) is only 3%. The slope of simulated curve
412 increases slightly after 2008 when the LAI continues to increase and NPP reaches a high level
413 (Fig. 3). The harvest records also show the same pattern after 2008 when heavy fertilization
414 began (456 kg N/ha/yr).

415 The per-month harvest records exhibit strong zig-zag pattern (Fig. 7). One reason is that oil
416 palms are harvested every 15-20 days and summarizing harvest events by calendar month
417 would result in uneven harvest times per month, e.g. two harvests fall in a previous month and
418 only one in the next month. Yet it still shows that harvests at PTPN-VI plantation dominated
419 from October to December whereas in the earlier months of each year harvest amounts were
420 significantly lower. The simulated amount of yield per harvest event has less seasonal
421 fluctuation, but it responds to the drought periods (Fig. 7). A slight positive linear correlation
422 exists between simulated yield and the mean precipitation of a 60-day period (corresponds to
423 the main fruit-filling and oil synthesis period) before each harvest event (Pearson's $r = 0.15$).

424 **4.2. Sensitivity analysis**

425 The leaf nitrogen fraction in Rubisco (F_{LNR}) is shown to be the most sensitive parameter (Fig.
426 8), because it determines the maximum rate of carboxylation at 25 °C (V_{cmax25}) together with
427 SLA (also sensitive), foliage nitrogen concentration (CN_{leaf} , Table A3) and other constants.
428 Given the fact that F_{LNR} should not vary widely in nature for a specific plant, we constrained
429 this parameter within narrow boundaries to get a V_{cmax25} around 100, which is similar to that
430 shared by all other crop PFTs (100.7) and higher than forests (around 60) in CLM. We fixed
431 SLA to 0.013 by field measurements. The value is only representative of the photosynthetic
432 leaflets. The initial root allocation ratio (a_{root}^i) has considerable influence on yield because it
433 modifies the overall respiration cost along the gradual declining trend of fine root growth
434 across 25 years (Eq. 1). The final ratio (a_{root}^f) has limited effects because its baseline value
435 (0.1) is set very low and thus the percentage changes are insignificant. The leaf allocation

436 coefficients (f_{leaf}^i, a_{leaf}^f) are very sensitive parameters because they determine the
437 magnitudes of LAI and GPP and consequently yield. The coefficients d_{mat} and d_{alloc}^{leaf} control
438 the nonlinear curve of leaf development (Eq. 4) and hence the dynamics of NPP and that
439 partitioned to fruits. They were calibrated to match both the LAI and yield dynamics.
440 Increased F_{stem}^{live} results in higher proportion of live stem throughout life, given the fixed stem
441 turnover rate, and therefore it brings higher respiration cost and lower yield. Decreasing the
442 fruit allocation coefficient a results in a higher base rate of A_{fruit} according to Eq. 5, whereas
443 increasing coefficient b brings up the rate of change and final magnitude of A_{fruit} if NPP
444 rises continuously. Their relative influence on yield is lower than the leaf allocation
445 coefficients because of the restriction by NPP dynamics (Eq. 5). Parameters lf_{disp} and
446 $transplant$ have negligible effects. lf_{disp} has to work together with the phenological parameter
447 GDD_{exp} to give a reasonable size of spear leaves before expansion according to field
448 observation. Varying the size of seedlings at transplanting by 10% or 30% does not alter the
449 final yield, likely because the resulting initial LAI is still within a limited range (0.1~0.2)
450 given the baseline value 0.15.

451 **4.3. Model validation with independent dataset**

452 The LAI development curves for the eight oil palm sites follow similar patterns since field
453 transplanting in different years (Fig. 9a). The average LAI of the eight sites from the model is
454 comparable with field measurement in 2014 (MPE = 10%, Fig. 9b). Small-scale variability
455 from site to site is not well captured, given that microclimate was only prescribed as two
456 categories for H and P plots respectively and all the plots followed the same fertilization
457 subroutine in the model. There are large uncertainties in field LAI estimates because we did
458 not measure LAI at the plot level directly but only sampled leaf area and dry weight of
459 individual phytomers and scaled the values up.

460 The simulated annual yields match closely with the average yield of the eight sites measured
461 in 2013-2014 (MPE = -4%) but the model-predicted variability across the sites is much lower
462 than field records (Fig. 10). Modelled yield generally increases with plantation age, which can
463 be explained by the increasing fruit allocation rate A_{fruit} with increasing LAI and NPP (Fig.
464 3). We do not have data to test an aging decline function of growth and yield and assume the
465 oil palm plantations remain productive for 25 years (Age_{max}) before replanting.

466 The simulated monthly NPP with the calibrated parameters for PTPN-VI site also closely
467 corresponds to the average level of field measured NPP from the 8 independent validation
468 sites with mature oil palms (Fig. 3).

469 **5. Discussion**

470 Calibration and validation with multiple site data demonstrate the utility of CLM-Palm and
471 the sub-canopy structure for simulating the growth and yield of the unique oil palm plantation
472 system within a land surface modeling context.

473 The pre-expansion phenological phase is proved necessary for simulating both phytomer-
474 level and PFT-level LAI development in a prognostic manner. The leaf C storage pool
475 provides an efficient buffer to support phytomer development and maintain overall LAI
476 during fruiting. It also avoids an abnormally fast increase of LAI in the juvenile stage when C
477 and N allocation is dedicated to the vegetative components. Without the leaf storage pool, the
478 plant's canopy develops unrealistically fast at young age and then enters an emergent drop
479 once fruit-fill begins (Fig. 4). This is because the plant becomes unable to sustain leaf growth
480 just from its current photosynthetic assimilates when a large portion is allocated to fruits.
481 Furthermore, differentiating the two phases could avoid abrupt increase in photosynthesis if a
482 phytomer with full dry mass shifts from photosynthetically inactive to active status at one step.
483 For the similar purpose, we implement the leaf senescence phenology phase which gradually

484 decreases the photosynthetic capacity of a leaf at the bottom layer of canopy so as to avoid
485 drastic reduction in photosynthesis if the bottom leaves were turned off immediately.

486 Resource allocation patterns for perennial crops are more difficult to simulate than annual
487 crops. For annuals, the LAI is often assumed to decline during grain-fill (Levis et al., 2012).
488 However, the oil palm has to sustain a rather stable leaf area while partitioning a significant
489 amount of C to the fruits. The balance between reproductive and vegetative allocations is
490 crucial. The dynamics of A_{fruit} as a function of monthly NPP is meant to capture the
491 increasing yield capacity of oil palms during maturing at favorable conditions (often the case
492 in oil palm plantations). The average value of A_{fruit} was around 1 (Fig. 3), resulting a near 1:1
493 ratio to partition available assimilates to the reproductive and vegetative pools which matched
494 closely with field observations (Kotowska et al., 2015a; Kotowska et al., 2015b). Under
495 severe stress conditions, this NPP-related function can decrease fruit allocation and shift
496 resources to the vegetative components. Our experiments (not shown here) confirmed that the
497 dynamic function is more robust than a simple time-dependent or vegetation-size-dependent
498 allocation function. Figure 3 also shows that the average rate of growth and productivity (NPP)
499 of mature oil palms is reasonably captured by the model across different site conditions.

500 The phenology and allocation processes in land surface models are usually aimed to represent
501 the average growth trend of a PFT at large spatial scale (Bonan et al., 2002; Drewniak et al.,
502 2013). We made a step forward by comparing point simulations with multiple specific site
503 observations. The model predicts well the average LAI development and yield across the
504 Jambi region as well as monthly NPP of mature plantations. Yet it exhibits a limitation of the
505 land surface modeling approach, that is, the difficulty to capture the large site-to-site
506 variations. The discrepancy was very likely due to insufficient representation of management
507 (e.g. fertilization, harvest and pruning cycles), which has been shown to be crucial for
508 determining oil palm growth and yield (Euler et al., 2015). Other factors such as insects,
509 fungal infection, and possibly different oil palm progenies could also result in difference in

510 the average size and number of leaves and fruits per palm, and they are not represented in the
511 model. Water availability (precipitation) and soil condition were only prescribed as two
512 categories of inputs for H and B plots, respectively. Especially the amount and timing of
513 fertilization vary largely from plantation to plantation and from year to year but the model
514 uses uniform fertilization for all plots (which is usually the case when modeling with a PFT).
515 A more complex dynamic fertilization scheme could be devised and evaluated thoroughly
516 with additional field data, which we lack at the moment.

517 The seasonal variability in yield simulated by the model well corresponds to precipitation data
518 but it is difficult to interpret the difference with harvest records due to the artificial zig-zag
519 pattern. The harvest records from plantations do not necessarily correspond to the amount of
520 mature fruits along a phenological time scale due to varying harvest arrangements, e.g. fruits
521 are not necessarily harvested when they are ideal for harvest, but when it is convenient.
522 Observations of mature fruits on a tree basis (e.g. Navarro et al., 2008 on coconut) would be
523 more suitable to compare with modeled yield, but such data are not available at our sites.
524 Some studies have also demonstrated important physiological mechanisms on oil palm yield
525 including inflorescence gender determination and abortion rates that both respond to seasonal
526 climatic dynamics although with a time lag (Combres et al., 2013; Legros et al., 2009). The
527 lack of representation of such physiological traits might affect the seasonal dynamics of yield
528 simulated by our model. However, these mechanisms are rarely considered in a land surface
529 modelling context.

530 Nevertheless, the sub-canopy phytomer-based structure, the extended phenological phases for
531 a perennial crop PFT and the two-step allocation scheme are distinct from existing functions
532 in land surface models. The phytomer configuration of CLM-Palm is similar to the one
533 already implemented in other oil palm growth and yield models such as the APSIM-Oil Palm
534 model (Huth et al., 2014) or the ECOPALM yield prediction model (Combres et al., 2013).
535 But the implementation of this sub-canopy structure is the first attempt among land surface

536 models. CLM-Palm incorporates the ability of yield prediction, like an agricultural model,
537 beside that it allows the modeling of biophysical and biogeochemical processes as a land
538 model should do, e.g. what is the whole fate of carbon in plant, soil and atmosphere if land
539 surface composition changes from a natural system to the managed oil palm system? In a
540 following study, a fuller picture of the carbon, water and energy fluxes over the oil palm
541 landscape are examined with the CLM-Palm sub-model presented here and evaluated with
542 Eddy Covariance flux observation data. We develop this palm module in the CLM framework
543 as it allows coupling with climate models so that the feedbacks of oil palm expansion to
544 climate can be simulated in future steps.

545 **6. Conclusions**

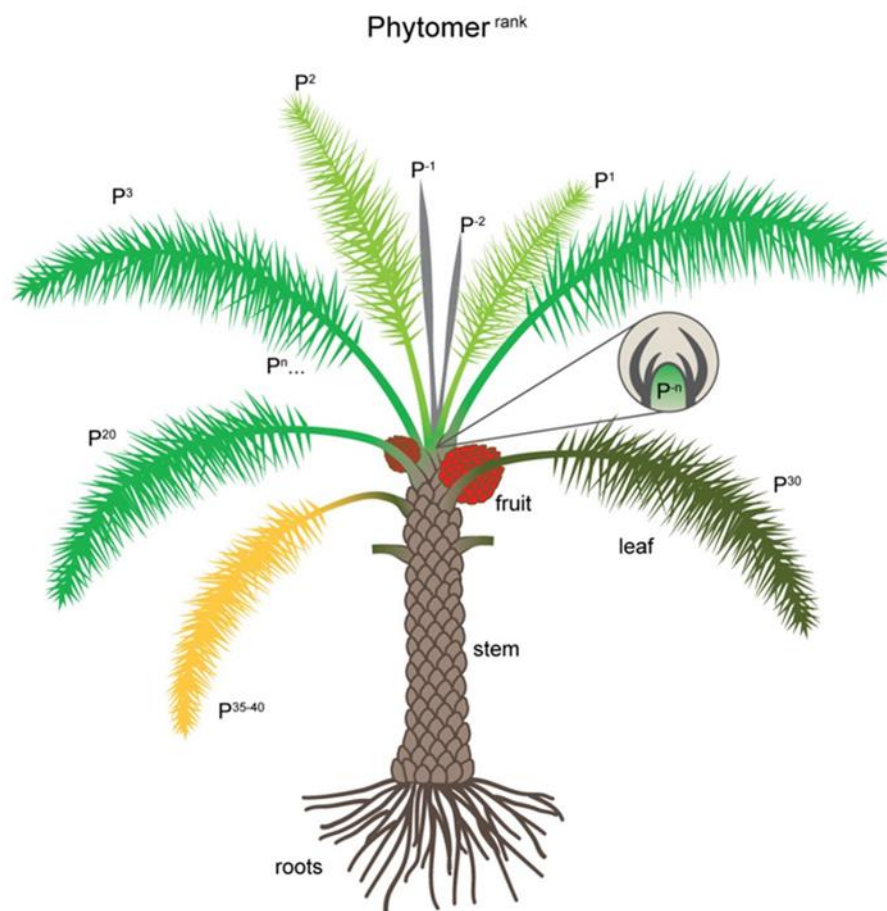
546 The development of CLM-Palm including canopy structure, phenology, and carbon and
547 nitrogen allocation functions was proposed for modeling an important agricultural system in
548 Indonesia. This paper demonstrates the ability of the new palm module to simulate the inter-
549 annual dynamics of vegetative growth and fruit yield from field planting to full maturity of
550 the plantation. The sub-canopy-scale phenology and allocation strategy are necessary for this
551 perennial evergreen crop which yields continuously on multiple phytomers. The pre-
552 expansion leaf storage growth phase is proved essential for buffering and balancing overall
553 vegetative and reproductive growth. Average LAI, yield and NPP were satisfactorily
554 simulated for multiple sites, which fulfills the main mission of a land surface modeling
555 approach, that is, to represent the average conditions and dynamics of large-scale processes.
556 On the other hand, simulating small-scale site-to-site variation (50m × 50m sites) requires
557 detailed input data on site conditions (e.g. microclimate, soil, and micro-topography) and
558 plantation managements that are often not available thus limiting the applicability of the
559 model at small scale. The point simulations here provide a starting point for calibration and
560 validation at large scales.

561 To be run in a regional or global grid, the age class structure of plantations needs to be taken
562 into account. This can be achieved by setting multiple replicates of the PFT for oil palm, each
563 planted at a point of time at a certain grid. As a result, a series of oil palm cohorts developing
564 at different grids could be configured with a transient PFT distribution dataset, which allows
565 for a quantitative analysis of the effects of land-use changes, specifically rainforest to oil palm
566 conversion, on carbon, water and energy fluxes. This will contribute to the land surface
567 modeling community for simulating this structurally unique, economically and ecologically
568 sensitive, and fast expanding oil palm land cover.

569 **Acknowledgements:**

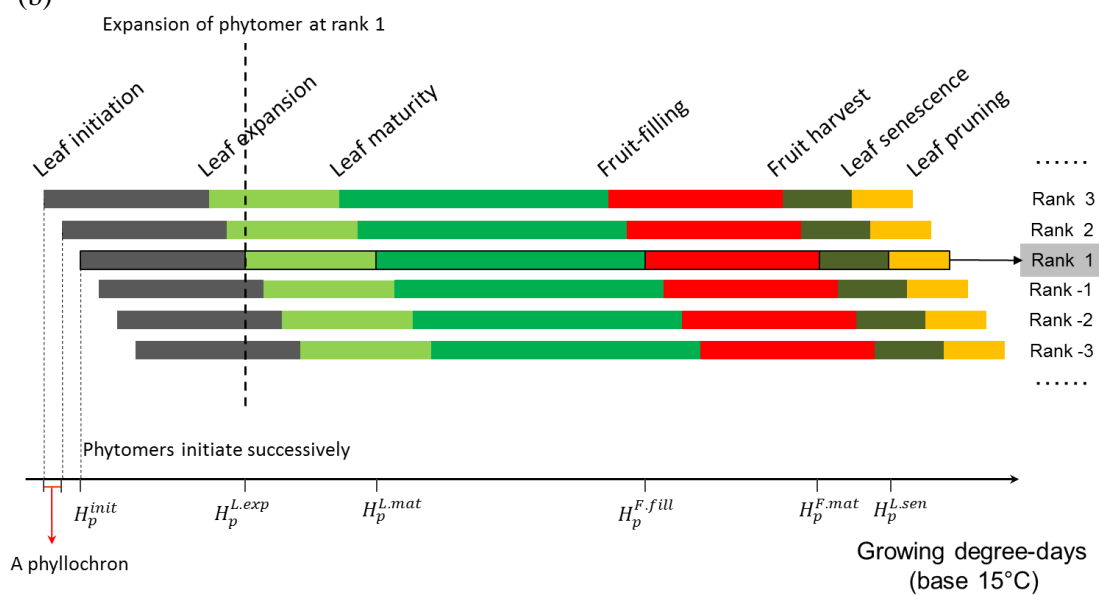
570 This study was funded by the European Commission Erasmus Mundus FONASO Doctorate
571 fellowship. Field trips were partly supported by the Collaborative Research Centre 990
572 (Ecological and Socioeconomic Functions of Tropical Lowland Rainforest Transformation
573 Systems (Sumatra, Indonesia)) funded by the German Research Foundation (DFG). We are
574 grateful to Kara Allen (University of Göttingen, Germany), Dr. Bambang Irawan (University
575 of Jambi, Indonesia) and the PTPN-VI plantation in Jambi for providing field data on oil palm.
576 The source code of the post-4.5 version CLM model was provided by Dr. Samuel Levis from
577 National Center for Atmospheric Research (NCAR), Boulder, CO, USA.

(a)



579

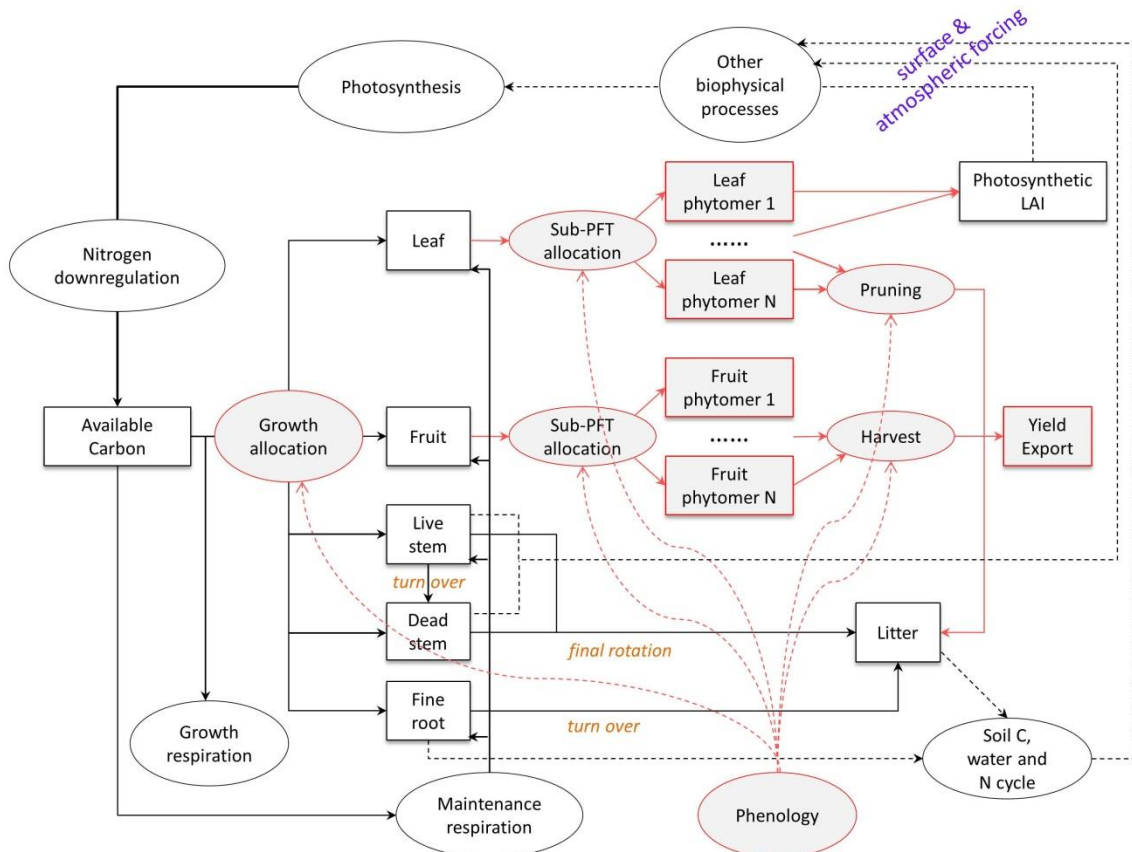
(b)



580

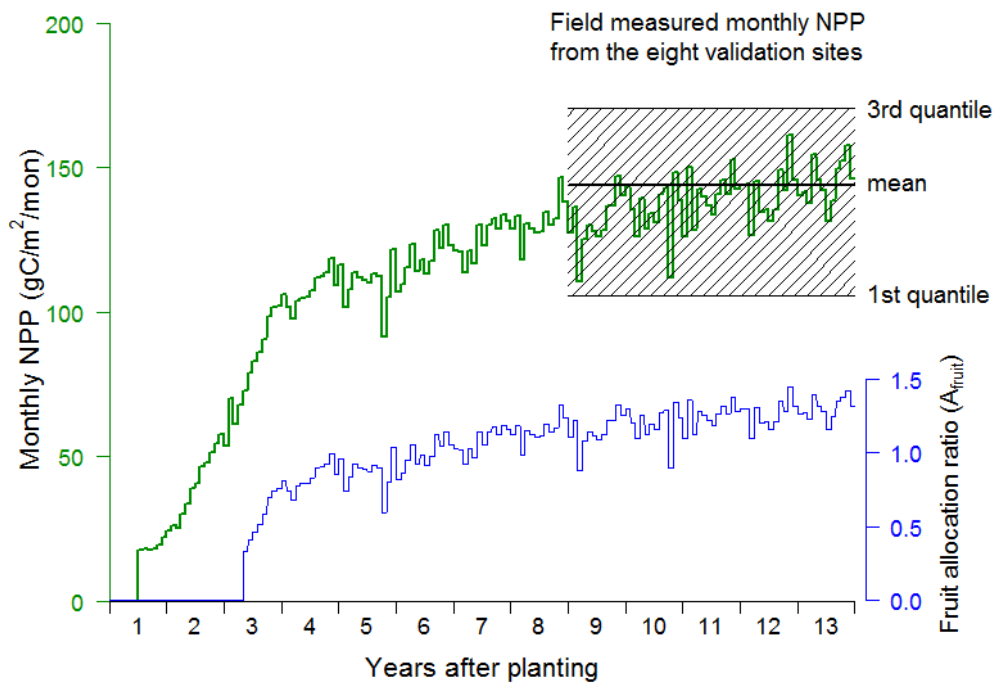
581 Fig. 1. (a) New sub-canopy phytomer structure for oil palm within CLM-Palm. P^1 to P^n
 582 indicate expanded phytomers and P^{-1} to P^{-n} at the top indicate unexpanded phytomers packed
 583 in the bud. Each phytomer has its own phenology, represented by different colors
 584 corresponding to: (b) the phytomer phenology: from initiation to leaf expansion, to leaf
 585 maturity, to fruit-fill, to harvest, to senescence and to pruning. Phytomers initiate successively
 586 according to the phyllochron (the period in heat unit between initiations of two subsequent
 587 phytomers). Detailed phenology description is in Supplementary materials.

588



589

590 Fig. 2. Original and modified structure and functions for developing CLM-Palm in the
 591 framework of CLM4.5. Original functions from CLM4.5 are represented in black. New
 592 functions designed for CLM-Palm are represented in red, including phenology,
 593 pruning, fruit harvest and export, as well as the sub-canopy structure.

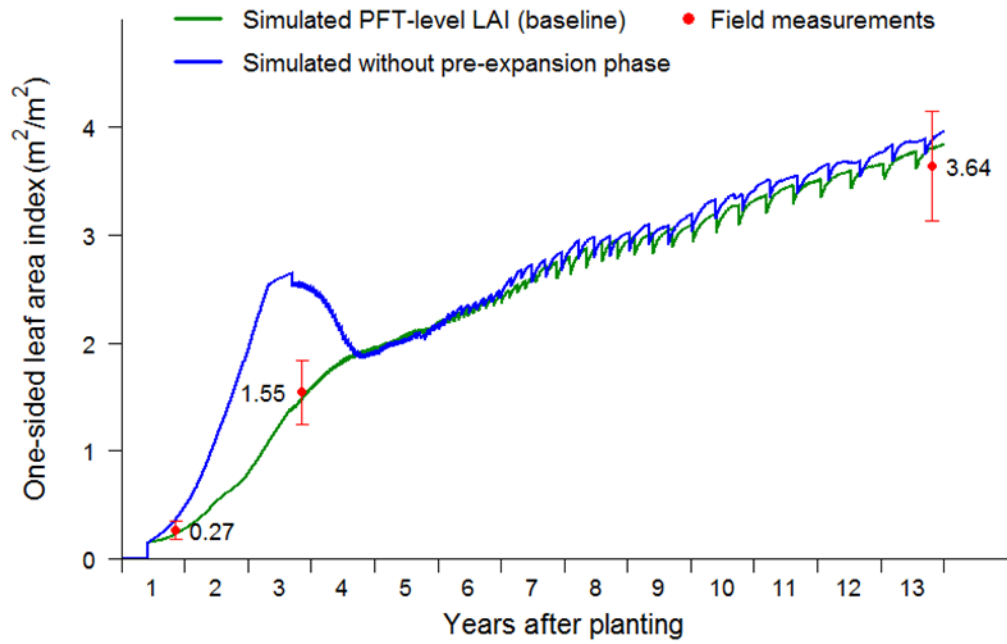


594

595 Fig. 3. Time course of reproductive allocation rate (blue line) in relation to monthly NPP from
 596 the previous month (NPP_{mon} , green line) according to Eq. 5. A_{fruit} is relative to the vegetative
 597 unity ($A_{leaf} + A_{stem} + A_{root} = 1$ and $0 \leq A_{fruit} \leq 2$). The NPP_{mon} was simulated with
 598 calibrated parameters for the PTPN-VI site and was compared with field measured monthly
 599 NPP from the 8 validation sites in Harapan and Bukit Duabelas regions.

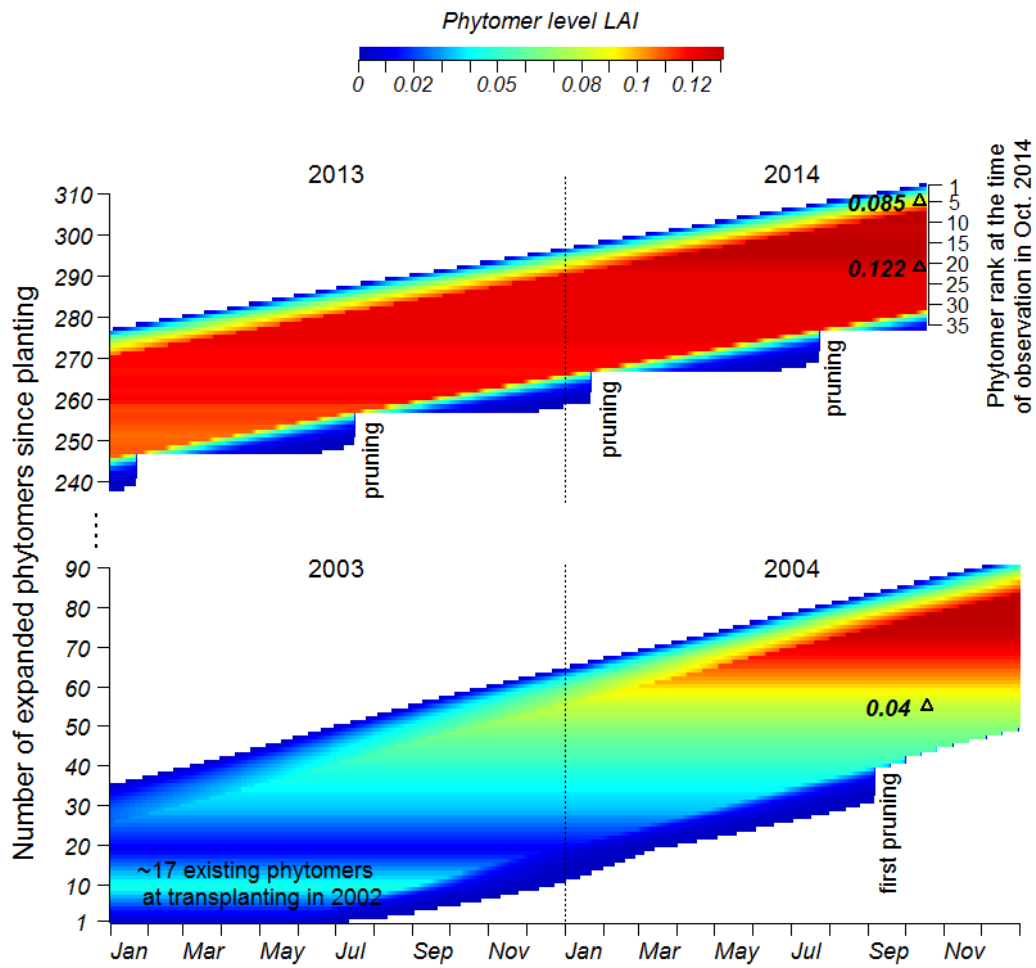
600

601



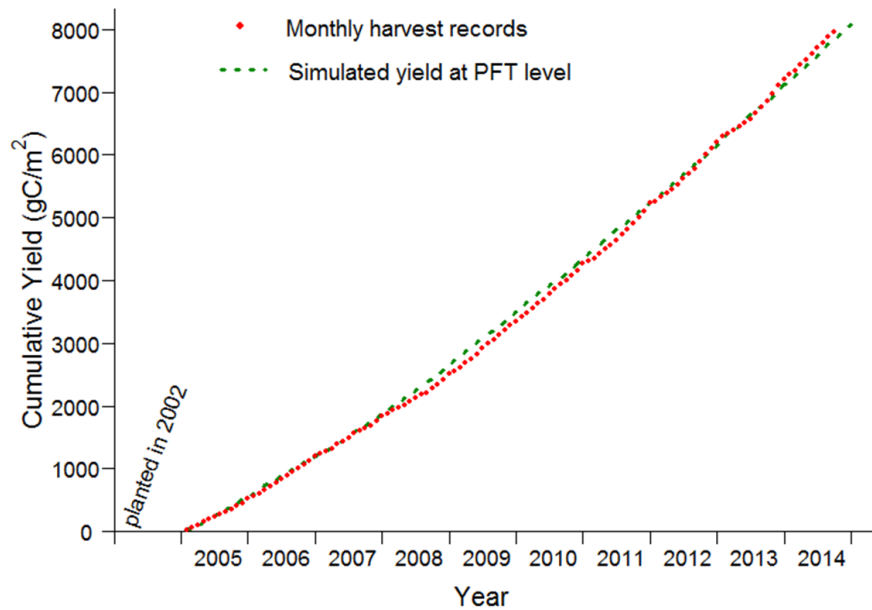
602

603 Fig. 4. PFT-level LAI simulated by CLM-Palm, with and without the pre-expansion growth
 604 phase in the phytomer phenology and compared to field measurements used for calibration.
 605 The initial sudden increase at year 1 represents transplanting from nursery. The sharp drops
 606 mark pruning events.



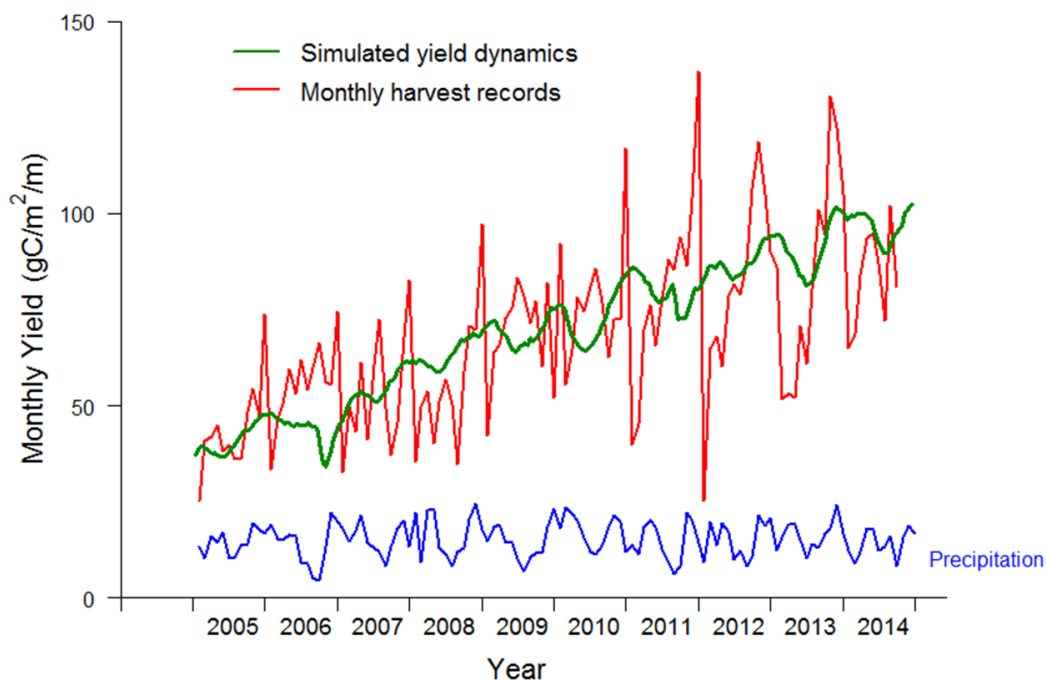
607

608 Fig. 5. Simulated phytomer level LAI dynamics (horizontal color bar) compared with field
 609 observations (black triangles with measured LAI value). The newly expanded phytomer at a
 610 given point of time has a rank of 1. Each horizontal bar represents the life cycle of a phytomer
 611 after leaf expansion. Phytomers emerge in sequence and the y-axis gives the total number of
 612 phytomers that have expanded since transplanting in the field. Senescent phytomers are
 613 pruned.



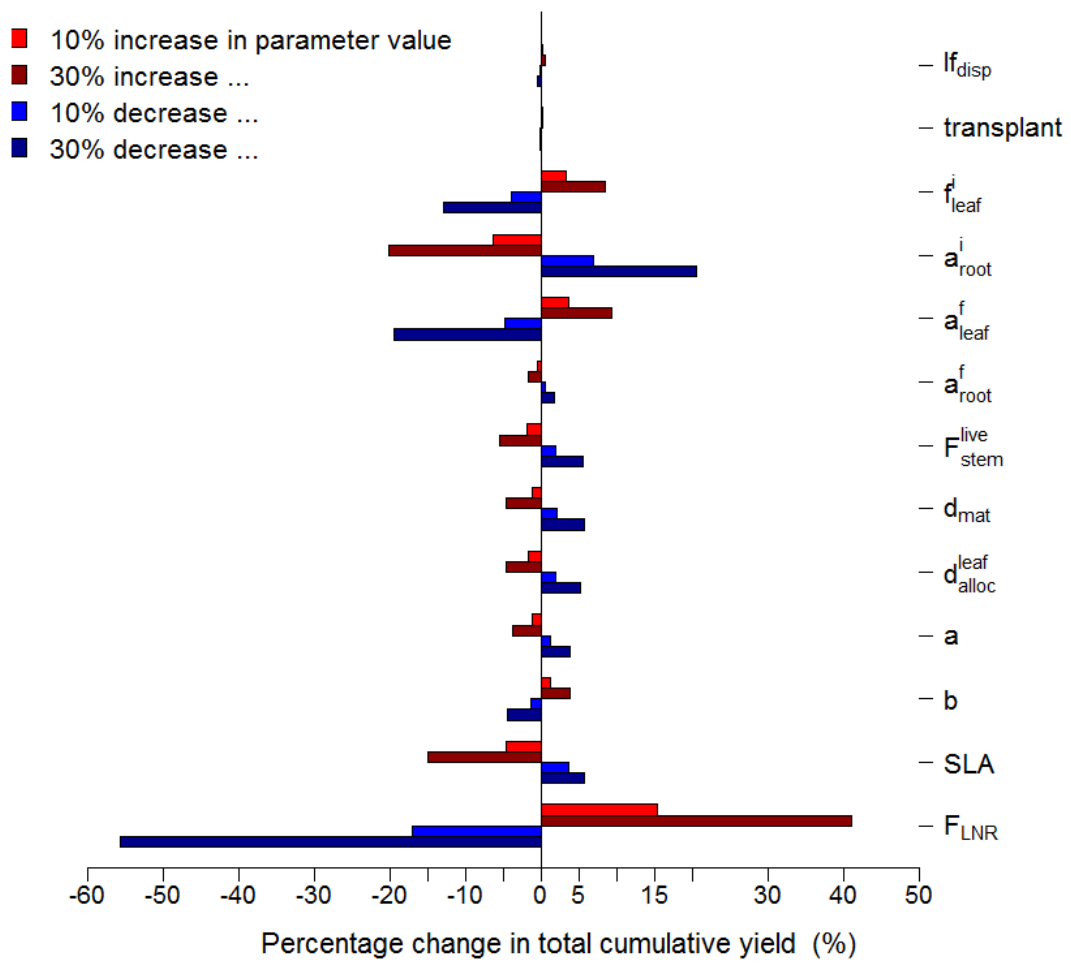
614

615 Fig. 6. Simulated PFT-level yield compared with monthly harvest data (2005-2014) from the
 616 calibration site PTPN-VI in Jambi, Sumatra. CLM-Palm represents multiple harvests (about
 617 twice per month) from different phytomers throughout time. The cumulative harvest amount
 618 from the model matches well with field records (MPE = 3%).



619

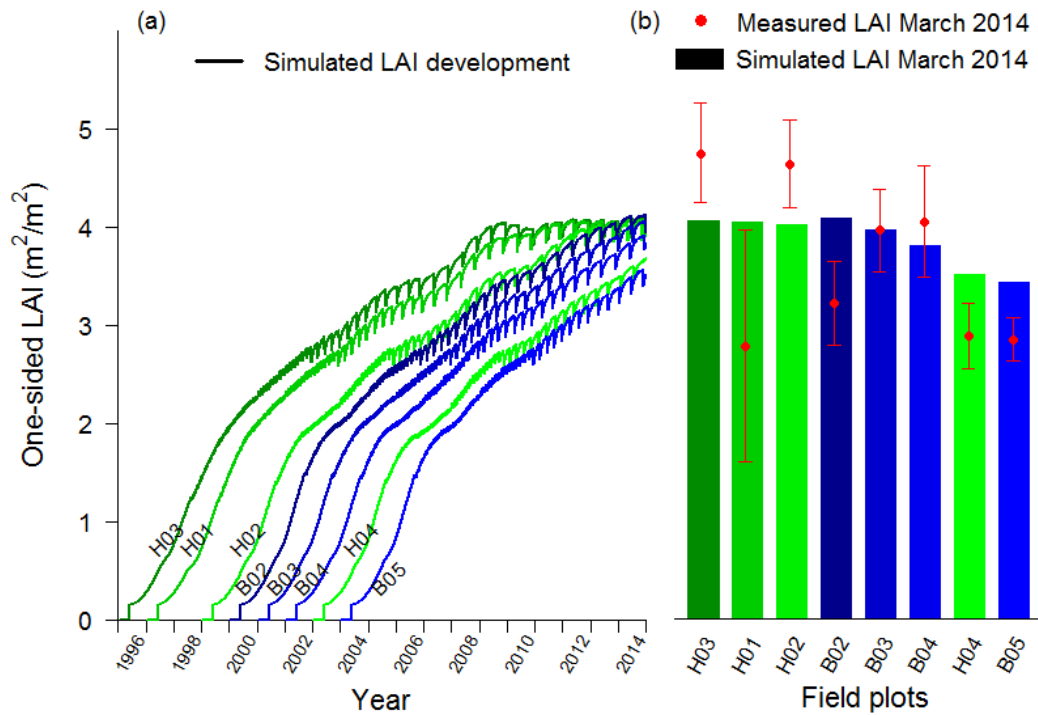
620 Fig. 7. Simulated and observed monthly yield at PTPN-VI compared with precipitation data.
 621 The modeled yield outputs are per harvest event (every 15-20 days depending on the
 622 phyllochron), while harvest records are the summary of harvest events per month. The model
 623 output is thus rescaled to show the monthly trend of yield that matches the mean of harvest
 624 records, given that the cumulative yields are almost the same between simulation and
 625 observation as shown in Fig. 6.



626

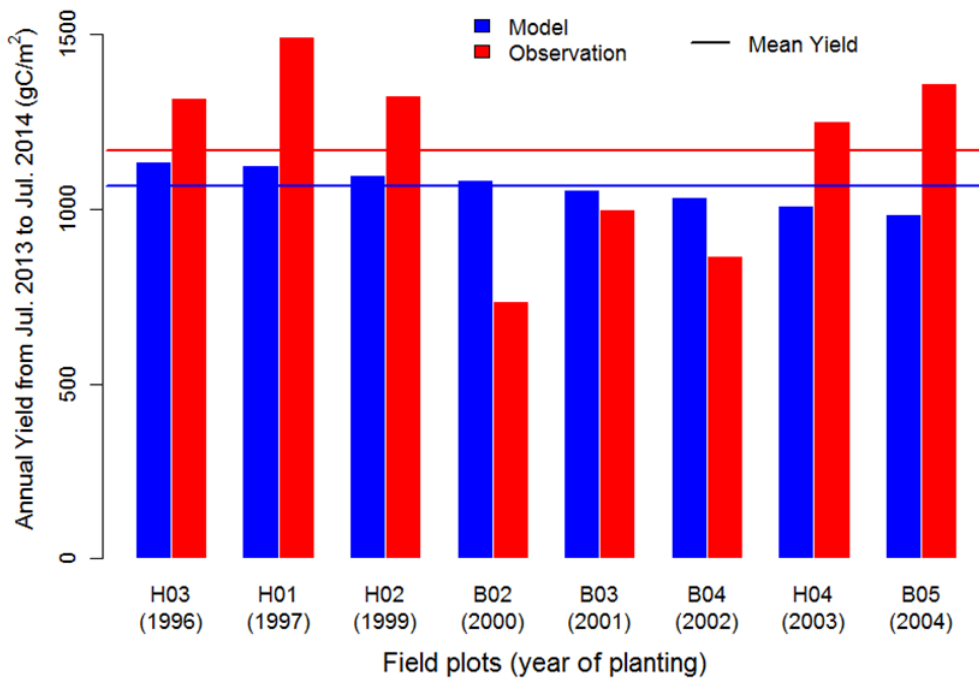
627 Fig. 8. Sensitivity analysis of key allocation parameters in regard of the cumulative yield at
 628 the end of simulation, with two magnitudes of change in the value of a parameter one-by-one
 629 while others are hold at the baseline values in Table A2.

630



631

632 Fig. 9. Validation of LAI with 8 independent oil palm sites (sequence in plantation age) from
 633 the Harapan (H) and Bukit Duabelas (B) regions: (a) shows the LAI development of each site
 634 simulated by the model since planting; (b) shows the comparison of field measured LAI in
 635 2014 with model.



636

637 Fig. 10. Validation of yield with 8 independent oil palm sites from the Harapan (H) and Bukit
 638 Duabelas (B) regions. The model predicted mean yield matches well with site average but
 639 site-to-site variability due to management difference was not reflected by simulation.

640 **Appendix A**

641 Summary of main parameters

642 Table A1. Summary of new phenological parameters introduced for oil palm in the phenology subroutine. The default values were determined by calibration
 643 and with reference to field observations and literatures on oil palm (Combres et al., 2013; Corley and Tinker, 2003; Hormaza et al., 2012; Legros et al., 2009).

Parameter	Default	Min	Max	Explanation (Unit)
<i>GDD_{init}</i>	0	0	1500	GDD needed from planting to the first phytomer initiation (°days). Initiation refers to the start of active accumulation of leaf C. A value 0 implies transplanting.
<i>GDD_{exp}</i>	1550	0	8000	GDD needed from leaf initiation to start of leaf expansion for each phytomer (pre-expansion) (°days)
<i>GDD_{L.mat}</i>	1250	500	1600	GDD needed from start of leaf expansion to leaf maturity for each phytomer (post-expansion) (°days)
<i>GDD_{F.fill}</i>	3800	3500	4200	GDD needed from start of leaf expansion to beginning of fruit-fill for each phytomer (°days)
<i>GDD_{F.mat}</i>	5200	4500	6500	GDD needed from start of leaf expansion to fruit maturity and harvest for each phytomer (°days)
<i>GDD_{L.sen}</i>	6000	5000	8000	GDD needed from start of leaf expansion to beginning of senescence for each phytomer (°days)
<i>GDD_{end}</i>	6650	5600	9000	GDD needed from start of leaf expansion to end of senescence for each phytomer (°days)
<i>GDD_{min}</i>	7500	6000	10000	GDD needed from planting to the beginning of first fruit-fill (°days)
<i>Age_{max}</i>	25	20	30	Maximum plantation age (productive period) from planting to final rotation /replanting (years)
<i>mxlivenp</i>	40	30	50	Maximum number of expanded phytomers coexisting on a palm
<i>phyllochron</i>	130	100	160	Initial phyllochron (=plastochron): the period in heat unit between the initiations of two successive phytomers. The value increases to 1.5 times, i.e. 195, at 10-year old (°days)

644

645 Table A2. Summary of parameters involved in C and N allocation. The default values were determined by calibration and with reference to field
 646 measurements (Kotowska et al., 2015a).

Parameter	Defaults	Min	Max	Explanation (Unit)
$*f_{disp}$	0.3	0.1	1	Fraction of C and N allocated to the displayed leaf pool
$*transplant$	0.15	0	0.3	Initial total LAI assigned to existing expanded phytomers at transplanting. Value 0 implies planting as seeds.
f_{leaf}^i	0.16	0	1	Initial value of leaf allocation coefficient before the first fruit-fill
a_{root}^i	0.3	0	1	Initial value of root allocation coefficient before the first fruit-fill
a_{leaf}^f	0.27	0	1	Final value of leaf allocation coefficient after vegetative maturity
a_{root}^f	0.1	0	1	Final value of root allocation coefficient after vegetative maturity
F_{stem}^{live}	0.15	0	1	Fraction of new stem allocation that goes to live stem tissues, the rest to metabolically inactive stem tissues
d_{mat}	0.5	0.1	1	Factor to control the age when the leaf allocation ratio stabilizes at a_{leaf}^f according to Eq. 4
d_{alloc}^{leaf}	0.6	0	5	Factor to control the nonlinear function in Eq. 4. Values < 1 give a convex curve and those > 1 give a concave curve. Value 1 gives a linear function.
$*a$	0.28	0	1	Parameter a for fruit allocation coefficient A_{fruit} in Eq. 5
$*b$	0.03	0	1	Parameter b for fruit allocation coefficient A_{fruit} in Eq. 5
$PLAI_{max}$	0.165	0.1	0.2	Maximum LAI of a single phytomer ($m^2 m^{-2}$)
SLA	0.013	0.01	0.015	Specific leaf area ($m^2 g^{-1} C$)
F_{LNR}	0.0762	0.05	0.1	Fraction of leaf nitrogen in Rubisco enzyme. Used together with SLA to calculate V_{cmax25} ($g N Rubisco g^{-1} N$)

647 *New parameters introduced for oil palm. Others are existing parameters in CLM but mostly are redefined or used in changed context.

648 Table A3. Other optical, morphological, and physiological parameters for oil palm.

Parameter	Value	Definition (Unit)	Comments
CN_{leaf}	25	Leaf carbon-to-nitrogen ratio (g C g ⁻¹ N)	Same as all other PFTs
CN_{root}	42	Root carbon-to-nitrogen ratio (g C g ⁻¹ N)	Same as all other PFTs
CN_{livewd}	50	Live stem carbon-to-nitrogen ratio (g C g ⁻¹ N)	Same as all other PFTs
CN_{deadwd}	500	Dead stem carbon-to-nitrogen ratio (g C g ⁻¹ N)	Same as all other PFTs
CN_{lfit}	50	Leaf litter carbon-to-nitrogen ratio (g C g ⁻¹ N)	Same as all other PFTs
CN_{fruit}	75	Fruit carbon-to-nitrogen ratio (g C g ⁻¹ N)	Higher than the value 50 for other crops because of high oil content in palm fruit
$r_{vis/nir}^{leaf}$	0.09/0.45	Leaf reflectance in the visible (VIS) or near-infrared (NIR) bands	Values adjusted in-between trees and crops
$r_{vis/nir}^{stem}$	0.16/ 0.39	Stem reflectance in the visible or near-infrared bands	Values adjusted in-between trees and crops
$\tau_{vis/nir}^{leaf}$	0.05/0.25	Leaf transmittance in the visible or near-infrared bands	Values adjusted in-between trees and crops
$\tau_{vis/nir}^{stem}$	0.001/ 0.001	Stem transmittance in the visible or near-infrared bands	Values adjusted in-between trees and crops
χ_L	0.6	Leaf angle index to calculate optical depth of direct beam (from 0 = random leaves to 1 = horizontal leaves; -1 = vertical leaves)	Average leaf angle according to field observation
$taper$	50	Ratio of stem height to radius-at-breast-height	Field observation. Used together with <i>stocking</i> and <i>dwood</i> to calculate canopy top and bottom heights.
<i>stocking</i>	150	Number of palms per hectare (stems ha ⁻²)	Field observation. Used to calculate stem area index (SAI) by: $SAI = 0.05 \times LAI \times stocking$.

<i>d_{wood}</i>	100000	Wood density (gC m ⁻³)	Similar as coconut palm (O. Roupsard, personal communication)
<i>R_{z0m}</i>	0.065	Ratio of momentum roughness length to canopy top height	T. June, personal communication
<i>R_d</i>	0.67	Ratio of displacement height to canopy top height	T. June, personal communication

- 650 Allen, K., Corre, M. D., Tjoa, A., and Veldkamp, E.: Soil nitrogen-cycling responses to
651 conversion of lowland forests to oil palm and rubber plantations in Sumatra, Indonesia,
652 PLoS ONE, 10(7), e0133325, doi:10.1371/journal.pone.0133325, 2015
- 653 Bilonis, I., Drewniak, B. A., and Constantinescu, E. M.: Crop physiology calibration in CLM,
654 Geoscientific Model Development, 8(4), 1071-1083, 2015.
- 655 Bonan, G. B., Levis, S., Kergoat, L., and Oleson, K. W.: Landscapes as patches of plant
656 functional types: An integrated concept for climate and ecosystem models, Global
657 Biogeochemical Cycles, 16 (2), 1021-1051, 2002.
- 658 Carlson, K. M., Curran, L. M., Asner, G. P., Pittman, A. M., Trigg, S. N., and Adeney, J. M.:
659 Carbon emissions from forest conversion by Kalimantan oil palm plantations, Nature
660 Clim. Change, 3(3), 283–287, doi:10.1038/nclimate1702, 2012.
- 661 Carrasco, L. R., Larrosa, C., Milner-Gulland, E. J., and Edwards, D. P.: A double-edged
662 sword for tropical forests, Science, 346(6205), 38-40, 2014.
- 663 Combres, J.-C., Pallas, B., Rouan, L., Mialet-Serra, I., Caliman, J.-P., Braconnier, S., Soulie,
664 J.-C., and Dingkuhn, M.: Simulation of inflorescence dynamics in oil palm and
665 estimation of environment-sensitive phenological phases: a model based analysis,
666 Functional Plant Biology, 40(3), 263-279, 2013.
- 667 Corley R. H. V. and Tinker, P. B. (Eds.): The oil palm, 4th edition, Blackwell Science,
668 Oxford, 2003.
- 669 Dee, D. P., Uppala, S. M., Simmons, A. J., Berrisford, P., Poli, P., Kobayashi, S., ... and
670 Vitart, F.: The ERA-Interim reanalysis: Configuration and performance of the data
671 assimilation system, Quarterly Journal of the Royal Meteorological Society, 137(656),
672 553-597, 2011.
- 673 Drewniak, B., Song, J., Prell, J., Kotamarthi, V. R., and Jacob, R.: Modeling agriculture in the
674 community land model, Geoscientific Model Development, 6(2), 495-515,
675 doi:10.5194/gmd-6-495-2013, 2013.
- 676 Euler, M.: Oil palm expansion among Indonesian smallholders - adoption, welfare
677 implications and agronomic challenges, Ph.D. thesis, University of Göttingen, Germany,
678 145 pp., 2015.
- 679 FAO. FAOSTAT Database, Food and Agriculture Organization of the United Nations, Rome,
680 Italy, available at: <http://faostat.fao.org/site/339/default.aspx> (last access: 17 June 2015),
681 2013.
- 682 Galloway, J. N., Dentener, F. J., Capone, D. G., Boyer, E. W., Howarth, R. W., Seitzinger, S.
683 P., ... and Vöösmary, C. J.: Nitrogen cycles: past, present, and future, Biogeochemistry,
684 70(2), 153-226, 2004.
- 685 Georgescu, M., Lobell, D. B., and Field, C. B.: Direct climate effects of perennial bioenergy
686 crops in the United States, Proceedings of the National Academy of Sciences, 108(11),
687 4307-4312, 2011.
- 688 Goh K. J.: Climatic requirements of the oil palm for high yields, in: Managing oil palm for
689 high yields: agronomic principles, Goh K.J. (Eds.), pp. 1–17, Malaysian Soc. Soil Sci.
690 and Param Agric. Surveys, Kuala Lumpur, 2000.
- 691 Gunarso, P., Hartoyo, M. E., Agus, F., and Killeen, T. J.: Oil Palm and Land Use Change in
692 Indonesia, Malaysia, and Papua New Guinea. In: Killeen T, Goon J, editors. Reports
693 from the Science Panel of the Second GHG Working Group of the Roundtable for
694 Sustainable Palm Oil (RSPO). Kuala Lumpur, 2013.
- 695 Hall é F., Oldeman, R. A. A. and Tomlinson, P. B.: Tropical trees and forests. An
696 architectural analysis. Springer-Verlag, Berlin, 441 pp., 1978.
- 697 Hijmans, R. J., Cameron, S. E., Parra, J. L., Jones, P. G., and Jarvis, A.: Very high resolution
698 interpolated climate surfaces for global land areas, International journal of climatology,
699 25(15), 1965-1978, 2005.
- 700 Hoffmann, M. P., Vera, A. C., Van Wijk, M. T., Giller, K. E., Oberthür, T., Donough, C., and
701 Whitbread, A. M.: Simulating potential growth and yield of oil palm (*Elaeis guineensis*)

702 with PALMSIM: Model description, evaluation and application, *Agricultural Systems*,
703 131, 1-10, 2014.

704 Hormaza, P., Fuquen, E. M., and Romero, H. M.: Phenology of the oil palm interspecific
705 hybrid *Elaeis oleifera* × *Elaeis guineensis*, *Scientia Agricola*, 69(4), 275-280, 2012.

706 Huth, N. I., Banabas, M., Nelson, P. N., and Webb, M.: Development of an oil palm cropping
707 systems model: lessons learned and future directions, *Environ. Modell. Softw.*, 62, 411–
708 419, doi:10.1016/j.envsoft.2014.06.021, 2014.

709 Jin, J. M. and Miller, N. L.: Regional simulations to quantify land use change and irrigation
710 impacts on hydroclimate in the California Central Valley, *Theoretical and Applied
711 Climatology*, 104, 429-442, 2011.

712 Koh, L. P. and Ghazoul, J.: Spatially explicit scenario analysis for reconciling agricultural
713 expansion, forest protection, and carbon conservation in Indonesia, *P. Natl. Acad. Sci.
714 USA*, 107, 11140–11144, doi: 10.1073/pnas.1000530107, 2010.

715 Kotowska, M. M., Leuschner, C., Antono, T., Meriem, S., and Hertel, D.: Quantifying
716 aboveand belowground biomass carbon loss with forest conversion in tropical lowlands
717 of Sumatra (Indonesia), *Global Change Biol.*, accepted, doi: 10.1111/gcb.12979, 2015a.

718 Kotowska, M. M., Leuschner, C., Triadiati, T., and Hertel, D.: Conversion of tropical lowland
719 forest lowers nutrient return with litterfall, and alters nutrient use efficiency and
720 seasonality of net primary productivity, *Oecologia*, submitted, 2015b.

721 Koven, C. D., Riley, W. J., Subin, Z. M., Tang, J. Y., Torn, M. S., Collins, W. D., Bonan, G.
722 B., Lawrence, D. M., and Swenson, S. C.: The effect of vertically resolved soil
723 biogeochemistry and alternate soil C and N models on C dynamics of CLM4,
724 *Biogeosciences*, 10(11), 7109-7131, doi:10.5194/bg-10-7109-2013, 2013.

725 Legros, S., Mialet-Serra, I., Caliman, J. P., Siregar, F. A., Clement-Vidal A., and Dingkuhn,
726 M.: Phenology and growth adjustments of oil palm (*Elaeis guineensis*) to photoperiod
727 and climate variability, *Annals of Botany* 104, 1171–1182. doi:10.1093/aob/mcp214,
728 2009.

729 Levis, S., Bonan, G., Kluzek, E., Thornton, P., Jones, A., Sacks, W., and Kucharik, C.:
730 Interactive crop management in the Community Earth System Model (CESM1):
731 Seasonal influences on land-atmosphere fluxes, *J. Climate*, 25, 4839-4859,
732 DOI:10.1175/JCLI-D-11-00446.1., 2012.

733 Luysaert, S., Schulze, E. D., Börner, A., Knohl, A., Hessenmdler, D., Law, B. E., Ciais, P.,
734 and Grace, J.: Old-growth forests as global carbon sinks, *Nature*, 455(7210), 213-215,
735 2008.

736 Miettinen, J., Shi, C. H. and Liew, S. C.: Deforestation rates in insular Southeast Asia
737 between 2000 and 2010, *Global Change Biology*, 17, 2261-2270, 2011.

738 Navarro, M. N. V., Jourdan, C., Sileye, T., Braconnier, S., Mialet-Serra, I., Saint-Andre, L., ...
739 and Rouspard, O.: Fruit development, not GPP, drives seasonal variation in NPP in a
740 tropical palm plantation, *Tree physiology*, 28(11), 1661-1674, 2008.

741 Oleson, K. W., Bonan, G. B., Levis, S., and Vertenstein, M.: Effects of land use change on
742 North American climate: impact of surface datasets and model biogeophysics, *Climate
743 Dynamics*, 23, 117-132, 2004.

744 Oleson, K., Lawrence, D., Bonan, G., Drewniak, B., Huang, M., Koven, C., Levis, S., Li, F.,
745 Riley, W., Subin, Z., Swenson, S., Thornton, P., Bozbiyik, A., Fisher, R., Heald, C.,
746 Kluzek, E., Lamarque, J.-F., Lawrence, P., Leung, L., Lipscomb, W., Muszala, S.,
747 Ricciuto, D., Sacks, W., Sun, Y., Tang, J., and Yang, Z.-L.: Technical description of
748 version 4.5 of the Community Land Model (CLM), National Center for Atmospheric
749 Research, Boulder, Colorado, USA, 420 pp., doi:10.5065/D6RR1W7M, 2013.

750 Tang, J. Y., Riley, W. J., Koven, C. D., and Subin, Z. M.: CLM4-BeTR, a generic
751 biogeochemical transport and reaction module for CLM4: model development,
752 evaluation, and application, *Geosci. Model Dev.*, 6, 127-140. doi:10.5194/gmd-6-127-
753 2013, 2013.

754 van Kraalingen, D. W. G., Breure, C. J., and Spitters, C. J. T.: Simulation of oil palm growth
755 and yield, *Agricultural and forest meteorology*, 46(3), 227-244, 1989.

756 Veldkamp, E., and Keller, M.: Nitrogen oxide emissions from a banana plantation in the
757 humid tropics, *Journal of Geophysical Research: Atmospheres* (1984–2012), 102(D13),
758 15889-15898, 1997.

759 von Uexküll, H., Henson, I.E., and Fairhurst, T.: Canopy management to optimize yield, in:
760 *Oil Palm: Management for Large and Sustainable Yields*, Fairhurst, T., and Hårdter, R.
761 (Eds.), Potash & Phosphate Institute of Canada, Potash & Phosphate Institute,
762 International Potash Institute, Singapore, pp. 163-180, 2003.

763 White, M. A., Thornton, P. E., and Running, S. W.: A continental phenology model for
764 monitoring vegetation responses to interannual climatic variability, *Global Biogeochem.*
765 *Cycles*, 11, 217-234, 1997.

766